$AVSeO_5$ (A = Rb, Cs) and $AV_3Se_2O_{12}$ (A = K, Rb, Cs, NH_4): Hydrothermal Synthesis in the V_2O_5−SeO_2−AOH System and Crystal Structure of $CsVSeO_5$

Young-Uk Kwon,* Kyu-Seok Lee, and Yoon Hyun Kim

Department of Chemistry, Sung Kyun Kwan University, Suwon 440-746, Korea

Received July 28, 1995[⊗]

Hydrothermal reactions in the V_2O_5−SeO_2−AOH systems (A = Na, K, Rb, Cs, NH_4) were studied with various reagent mole ratios. Typical millimole ratios were $V_2O_5/SeO_2/AOH = 5$ or $3/15/x$ in 10-mL aqueous solutions, where x was 5, 10, 15, and 20. The reactions with $x = 5$ for A = K, Rb, Cs, and NH_4 at 230 °C produced single-phase products of the general formula $AV_3Se_2O_{12}$ with the $(NH_4)(VO)_3(SeO_3)_2$ structure type. The $x = 15$ reactions for A = Rb and Cs yielded $AVSeO_5$ phases with a new structure type. The crystal structure for $CsVSeO_5$ was determined with X-ray single-crystal diffraction techniques to be monoclinic ($P2_1$ (No. 4), $a = 7.887(3)$ Å, $b = 7.843(2)$ Å, $c = 9.497(3)$ Å, $\beta = 92.13(3)°$, $Z = 4$). The structure of this compound consists of interwoven helixes extended in all three directions. The spires are composed of alternating SeO_3 and VO_5 units sharing common-edge oxygens in all three directions. For A = K and NH_4, the reactions of this mole ratio did not produce any identifiable phases. Each of the compounds is characterized by powder X-ray diffraction, infrared spectroscopic, and thermogravimetric techniques. The dependency of the synthesis results on the reaction conditions is discussed and rationalized.

Introduction

Many new solid state materials have been synthesized by hydrothermal reactions.[1] This technique is considered to have the potential of obtaining metastable materials with novel structures and unusual physical properties.[2] Unlike the traditional solid state reactions, this relatively low-temperature method depends on many variables such as concentration, mole ratio, pH, temperature, type of additive, and so forth. However, most of the papers mainly deal with the crystal structures and do not discuss much the synthetic conditions.

Interest in the synthesis of new transition metal selenite compounds has been increasing during the last few years.[3,4] Vanadium selenite compounds reported so far are VSe_2O_6,[3d] $VOSeO_3$,[3e] $VOSeO_3{\cdot}H_2O$,[5] $NH_4(VO)_3(SeO_3)_2$,[6] KV_2SeO_7,[7] and $Ba(VO)_2(SeO_3)_2(HSeO_3)_2$,[8] the last four of which having been synthesized from hydrothermal reactions. In the paper on NH_4-$(VO)_3(SeO_3)_2$, the authors reported their failed attempts to obtain alkali-metal analogs of this compound although their structure analysis indicated that the ammonium in $NH_4(VO)_3(SeO_3)_2$ could be replaced by alkai metals.[6] Since we have noted that reaction conditions are important to obtain pure compounds in the hydrothermal technique in the previous study on KV_2SeO_7,[7] we have investigated the V_2O_5−SeO_2−AOH (A = Na, K, Rb, Cs, NH_4) system under various reaction conditions, especially with various reagent mole ratios. During this study, we have obtained new compounds of two different structure types: $AVSeO_5$ (A = Rb, Cs), a new structure type, and $AV_3Se_2O_{12}$ (A = K, Rb, Cs), with the same crystal structure as $NH_4(VO_2)_3$-$(SeO_3)_2$. In this paper, we report the synthetic conditions and crystal structure for each of these compounds and other related phases.

Experimental Section

Synthesis. All the reactions in this study were carried out under hydrothermal conditions generated by autoclaves with Teflon liners. Measured amounts of reagents (V_2O_5, SeO_2, AOH powder or solution) were placed in an autoclave whose inside volume was 20 mL. Distilled water (about 10 mL) was added to make the degree of fill (volume ratio of the solution to the container) about 60%. The reaction vessels were placed in a convection oven equipped with a temperature controller so that the temperature inside the oven was constant within ± 0.5°C and uniform during the reactions. For the mole ratio effect study, we fixed the SeO_2 content at 15 mmol, fixed V_2O_5 at 3 or 5 mmol in the 10 mL solutions, and varied the content of AOH at 5, 10, 15, and 20 mmol. Typical reaction conditions and their results are listed in Table 1. The reaction numbers in the table will be used as identification codes in the following discussion.

Solid products were isolated from the solution via suction filtration, washed with distilled water, and air-dried. No changes in the solids upon exposure to air for months were observed. Except in a few cases, the products were composed of more than one phase. Separation of a phase from the intimately mixed mass was not possible. Phase identifications in such mixtures were therefore based upon microscopic observations of the crystal habits and color. Compounds obtained with high purity or single crystals that could be isolated were identified by their X-ray diffraction patterns (see below).

Single Crystal X-ray Structure Analysis. A platelike yellow crystal (0.6 × 0.8 × 0.2 mm) from reaction C-3 (Table 1) whose

[⊗] Abstract published in *Advance ACS Abstracts,* January 15, 1996.

(1) (a) Rabenau, A. *Angew. Chem., Int. Ed. Engl.* **1985**, *24*, 1026. (b) Davis, M. E.; Lobo, R. F. *Chem. Mater.* **1992**, *4*, 756.
(2) Gopalakrishinan, J. *Chem. Mater.* **1995**, *7*, 1265.
(3) Metal selenites from solid state syntheses: (a) Meunier, G.; Svensson, C.; Carry, A. *Acta Crystallogr.* **1976**, *B32*, 2664. (b) Bonvoisin, J.; Galy, J.; Trombe, J. C. *J. Solid State Chem.* **1993**, *107*, 171. (c) Meunier, G.; Bertaud, M. *Acta Crystallogr.* **1974**, *B30*, 2840. (d) Meunier, G.; Bertaud, M.; Galy, J. *Acta Crystallogr.* **1974**, *B30*, 2834. (e) Trombe, J.-C.; Gleizes, A.; Galy, J. *C. R. Acad. Sci., Ser. 2* **1983**, *297*, 667. (f) Trombe, J.-C.; Gleizes, A.; Galy, J.; Renard, J.-P.; Journaux, Y.; Verdaguer, M. *Nouv. J. Chim.* **1987**, *11*, 321.
(4) Metal selenites from hydrothermal reactions: (a) Wildner, M. *J. Solid State Chem.* **1993**, *103*, 341. (b) Wildner, M. *J. Solid State Chem.* **1994**, *113*, 252. (c) Giester, G.; Wildner, M. *J. Solid State Chem.* **1991**, *91*, 370. (d) Morris, R. E.; Wilkinson, A. P.; Cheetham, A. K. *Inorg. Chem.* **1992**, *31*, 4774. (e) Morris, R. E.; Cheetham, A. K. *Chem. Mater.* **1994**, *6*, 67. (f) Effenberger, H. *J. Solid State Chem.* **1987**, *70*, 303. (g) Morris, R. E.; Harrison, W. T. A.; Stucky, G. D.; Cheetham, A. K. *J. Solid State Chem.* **1991**, *94*, 227. (h) Giester, G. *J. Solid State Chem.* **1993**, *103*, 451.
(5) Huan, G.; Johnson, J. W.; Jacobson, A. J.; Goshorn, D. P. *Chem. Mater.* **1991**, *3*, 539.
(6) Vaughey, J. T.; Harrison, W. T. A.; Dussack, L. L.; Jacobson, A. J. *Inorg. Chem.* **1994**, *33*, 4370.
(7) Lee, K.-S.; Kwon, Y.-U.; Namgung, H.; Kim, S.-W. *Inorg. Chem.* **1995**, *34*, 4178.
(8) Harrison, W. T. A.; Vaughey, J. T.; Jacobson, A. J.; Goshorn, J. W. *J. Solid State Chem.* **1995**, *116*, 77.

0020-1669/96/1335-1161$12.00/0

Table 1. Hydrothermal Reaction Conditions and Results for the $V_2O_5-SeO_2-AOH$ System

A	reacn no.	amt (mmol) V_2O_5	amt (mmol) SeO_2	amt (mmol) AOH	temp (°C)	time (d)	results[a]
K	K-1	5	15	5	230	3	$KV_3Se_2O_{12}$ crystal (100)
	K-2	5	15	5	200	3	$KV_3Se_2O_{12}$ crystal, impurity
	K-3	5	15	10	230	3	$KV_3Se_2O_{12}$ crystal, brown mass
	K-4	5	15	15	230	3	brown mass, light green impurity
	K-5	3	15	10	230	2	$KV_3Se_2O_{12}$ crystals and powder
	K-6	3	15	15	230	3	brown mass, some gem chunks
Rb	R-1	5	15	5	230	3	$RbV_3Se_2O_{12}$ powder (100)
	R-2	5	15	10	230	3	$RbV_3Se_2O_{12}$ (90), $RbVSeO_5$ (10)
	R-3	5	15	15	230	5	$RbVSeO_5$ (20), $Rb_2V_6O_{16}$ (80)
	R-4	3	15	5	230	3	$RbV_3Se_2O_{12}$ (100)
	R-5	3	15	10	230	3	$RbVSeO_5$ microcrystals (100)
	R-6	3	15	15	230	5	$RbVSeO_5$ (20), $Rb_2V_6O_{16}$ (80)
Cs	C-1	5	15	5	230	3	$CsV_3Se_2O_{12}$ powder (100)
	C-2	5	15	10	230	3	$CsV_3Se_2O_{12}$ (90), $CsVSeO_5$ (10)
	C-3	5	15	15	230	4	$CsVSeO_5$ (60), $Cs_2V_6O_{16}$ (40)
	C-4	5	15	20	230	5	$CsVSeO_5$ (30), $Cs_2V_6O_{16}$ (70)
	C-5	3	15	10	230	3	$CsVSeO_5$ powder (100)
	C-6	3	15	15	230	3	$CsVSeO_5$ (50), $Cs_2V_6O_{16}$ (50)
NH_4	A-1	5	15	5	200	3	$NH_4V_3Se_2O_{12}$, green impurity
	A-2	5	15	5	230	5	$NH_4V_3Se_2O_{12}$ powder (100)
	A-3	5	15	15	230	5	cucumber green chunk

[a] Numbers in parentheses are estimated yields (%) based on visual inspections.

stoichiometry turned out to be $CsVSeO_5$ from this structure analysis was mounted on a glass fiber with epoxy. An Enraf-Nonius CAD4 diffractometer equipped with Mo Kα radiation (0.710 79 Å) was used for the data collection. Initial random search with the help of rotation photographs found 25 reflections which could be indexed with a monoclinic unit cell ($a = 7.887(3)$ Å, $b = 7.843(2)$ Å, $c = 9.497(3)$ Å, $\beta = 92.13(2)°$, $V = 587.1(3)$ Å^3). Data collection was performed on two octants ($\pm h, +k, +l$). The systematic extinction condition $0k0$ ($k = 2n + 1$) indicated the space groups $P2_1$ and $P2_1/m$. Both space groups were tried, and the former was found to be the correct one. In order to resolve the enantiomorphism of this noncentrosymmetric space group, a second data collection including four octants ($\pm h, \pm k, +l$) was performed and the refinements were made on this data set. The intensity data were corrected for the time decay and for Lorentz and polarization effects. Absorption corrections were made by the Gaussian integration method with nine faces measured (transmission coefficients: maximum, 0.0858; minimum, 0.0171; average, 0.0623). The SDP program package was used for the data set corrections.

The crystal structure was determined by direct methods with SHELXS-86,[9] and subsequent refinements and difference Fourier cycles were performed with SHELXL-93 based upon F^2 data.[10] The second-order extinction coefficients as well as anisotropic thermal parameters for all atoms were refined. One oxygen atom was refined non-positive definitely. Even though the absorption correction was already made with the Gaussian integration method, the rough surface, broken edges, and the high absorption coefficient of the crystal seemed to cause an uneven absorption correction. DIFABS[11] was, therefore, applied (corrections: minimum, 0.764; maximum, 1.134; average, 0.990), and the non-positive definite oxygen thermal parameter became positive in the following cycles of refinements. The full-matrix refinements converged to $R = 0.0229$ (on F) and $R_{2w} = 0.0602$ (on F^2) for all data. The present atomic parameters fitted the reflection data better than those of the other enantiomer (Flack x parameter[12] $= -0.002(5)$).

The crystal data are listed in Table 2, atomic positions and isotropic thermal parameters are given in Table 3, and important bond distances and angles are listed in Table 4.

Powder X-ray Diffractions. Apparently pure phase samples were analyzed by powder X-ray diffraction with a Rigaku D/Max-Rc diffractometer equipped with Ni-filtered Cu Kα radiation. The $K\alpha_2$ contribution to the diffraction patterns was eliminated by a stripping program, and the d values were calculated using the wavelength of the Cu $K\alpha_1$ line ($\lambda = 1.540\,56$ Å). Indexing of the powder patterns and least-squares refinements of the lattice parameters were performed using the parameters of the reported $NH_4V_3Se_2O_{12}$ and our $CsVSeO_5$ single-crystal structures.

Table 2. Crystallographic Data for $CsVSeO_5$

empirical formula	$CsVSeO_5$	T	23 °C
a	7.887(3) Å	space group	$P2_1$ (No. 4)
b	7.843(2) Å	λ	0.710 73 Å
c	9.497(3) Å	ρ_{calcd}	3.878 g/cm^3
b	92.13(3)°	μ	139.34 cm^{-1}
V	587.1(3) Å^3	R_1[a](F_o)	0.0229
Z	2	R_{2w}[b](F_o^2)	0.0602
fw	685.62		

[a] $R_1 = \Sigma||F_o|-|F_c||/\Sigma|F_o|$ [b] $R_{2w} = [\Sigma w(|F_o^2| - |F_c^2|)^2/\Sigma w|F_o^2|^2]^{1/2}$ with $w = 1/[\sigma^2(F_o^2) + (0.0392P)^2 + 1.49P]$, where $P = (F_o^2 + 2F_c^2)/3$.

Table 3. Atomic Coordinates ($\times 10^4$) and Equivalent Isotropic Displacement Parameters (Å$^2 \times 10^3$) for $CsVSeO_5$

	x	y	z	U_{eq}[a]
Cs(1)	−1263(1)	66(1)	−3869(1)	30(1)
Cs(2)	−5946(1)	−2613(1)	−1321(1)	27(1)
Se(1)	−6162(1)	3(1)	−5538(1)	17(1)
Se(2)	1193(1)	−7173(1)	−662(1)	18(1)
V(1)	−4187(2)	−2991(2)	−7312(1)	17(1)
V(2)	−720(2)	−4332(2)	−2357(1)	20(1)
O(1)	−4330(7)	1058(8)	−1732(6)	27(1)
O(2)	−3157(7)	−1621(7)	1219(6)	23(1)
O(3)	2546(8)	711(8)	−2880(7)	28(1)
O(4)	−4938(7)	1379(8)	−4562(6)	23(1)
O(5)	−4697(8)	−639(8)	−6668(6)	27(1)
O(6)	790(7)	−3315(9)	−3117(6)	31(1)
O(7)	835(8)	−1212(9)	−6912(7)	37(2)
O(8)	−9708(8)	−5180(8)	−594(6)	29(1)
O(9)	−1687(7)	−2514(8)	−1043(6)	26(1)
O(10)	−2788(7)	−3543(7)	−3411(6)	24(1)

[a] $U_{eq} = (U_1U_2U_3)^{1/3}$.

Infrared Spectroscopic and Thermogravimetric Measurements. Infrared spectra for the pure compounds were recorded with a Nicolet 205 spectrometer with KBr pellets in the frequency range 400−4000 cm^{-1}. Thermogravimetric measurements were performed with a Seiko TG/DTA 320 thermal analyzer under a N_2 flow up to 600 °C. The experimental weight loss (calculated value for total SeO_2 loss is given in parentheses) and the decomposition temperature range for each compound are as follows: in the $AV_3Se_2O_{12}$ series, 41.1% (41.0%) over 342−425 °C for A = K, 37.6% (37.7%) over 371−424 °C for Rb, and 34.7% (34.9%) over 385−428 °C for Cs compounds and 46.3%

(9) Sheldrick, G. M. SHELXS-86 User Guide. Crystallographic Department, University of Gottingen, Germany, 1985.
(10) Sheldrick, G. M. SHELXL-93 User Guide. Crystallographic Department, University of Gottingen, Germany, 1993.
(11) Walker, N.; Stuart, D. *Acta Crystallogr.* **1983**, *A39*, 158.
(12) Flack, H. D. *Acta Crystallogr.* **1983**, *A39*, 876.

Table 4. Important Bond Distances (Å) and Angles (deg) for $CsVSeO_5$

Cs(1)−O(7)	3.028(7)	Cs(2)−O(1)	3.082(6)
Cs(1)−O(10)	3.113(6)	Cs(2)−O(6)	3.084(6)
Cs(1)−O(4)	3.124(6)	Cs(2)−O(5)	3.099(6)
Cs(1)−O(3)	3.155(6)	Cs(2)−O(1)	3.179(6)
Cs(1)−O(6)	3.166(6)	Cs(2)−O(3)	3.205(7)
Cs(1)−O(6)	3.175(7)	Cs(2)−O(2)	3.224(5)
Cs(1)−O(1)	3.308(6)	Cs(2)−O(2)	3.297(6)
Cs(1)−O(9)	3.388(6)	Cs(2)−O(10)	3.323(6)
Cs(1)−O(7)	3.528(7)	Cs(2)−O(9)	3.361(6)
Cs(1)−O(5)	3.765(6)	Cs(2)−O(8)	3.672(6)
Se(1)−O(5)	1.684(6)	Se(2)−O(9)	1.672(5)
Se(1)−O(4)	1.700(5)	Se(2)−O(2)	1.712(5)
Se(1)−O(10)	1.709(5)	Se(2)−O(8)	1.720(6)
V(1)−O(1)	1.634(6)	V(2)−O(6)	1.624(6)
V(1)−O(3)	1.651(6)	V(2)−O(7)	1.631(7)
V(1)−O(2)	1.961(6)	V(2)−O(8)	1.945(6)
V(1)−O(5)	1.989(6)	V(2)−O(10)	1.981(6)
V(1)−O(4)	1.995(5)	V(2)−O(9)	2.060(6)
O(5)−Se(1)−O(4)	98.5(3)	O(9) −Se(2)−O(2)	99.2(3)
O(5)−Se(1)−O(10)	99.0(3)	O(9) −Se(2)−O(8)	101.0(3)
O(4)−Se(1)−O(10)	98.5(3)	O(2) −Se(2)−O(8)	99.3(3)
O(1) −V(1)−O(3)	108.8(3)	O(6)−V(2)−O(7)	106.6(4)
O(1) −V(1)−O(2)	99.3(3)	O(6)−V(2)−O(8)	105.4(3)
O(3) −V(1)−O(2)	94.2(3)	O(7) −V(2)−O(8)	94.1(3)
O(1) −V(1)−O(5)	116.5(3)	O(6)−V(2)−O(10)	103.1(3)
O(3) −V(1)−O(5)	134.8(3)	O(7) −V(2)−O(10)	92.0(3)
O(2) −V(1)−O(5)	78.7(2)	O(8) −V(2)−O(10)	147.7(3)
O(1) −V(1)−O(4)	96.8(3)	O(6)−V(2)−O(9)	102.9(3)
O(3) −V(1)−O(4)	92.5(3)	O(7) −V(2)−O(9)	150.2(3)
O(2) −V(1)−O(4)	159.5(3)	O(8) −V(2)−O(9)	82.2(2)
O(5)−V(1)−O(4)	82.8(2)	O(10)−V(2)−O(9)	76.9(2)

(3.3% for NH_3 plus 42.6% for SeO_2 losses, total 45.9%) over 104−456 °C for A = NH_4 (the two steps overlap); in the $AVSeO_5$ series, 36.6% (37.6%) over 382−539 °C for A = Rb and 31.6% (32.4%) over 390−517 °C for Cs compounds. The observed weight losses agreed well with the calculated ones within 1%.

Results and Discussion

Synthesis. In principle, the hydrothermal reaction technique has many variables that can influence the results significantly. Among these, we have considered the mole ratio (and pH) and the reaction temperature. Reaction time beyond 3 days does not seem to affect the final products significantly. Table 1 shows typical reaction conditions and their results. In order to see the effect of the relative concentration on the phase formation, we have varied the amount of AOH (A = Na, K, Rb, Cs, NH_4) while keeping those of V_2O_5 and SeO_2 fixed in most of the reaction runs. We did not try to adjust the pH because it was bound to change during reactions. The initial mixture in which V_2O_5 remained as a solid was very acidic with the pH below zero. As the reactions proceeded, V_2O_5 dissolved in the acidic solution to form VO_2^+ and the solution pH must rise according to the following reaction:[13]

$$V_2O_5 + 2H^+ \rightarrow 2VO_2^+ + H_2O$$

The final pH reached between 3 and 7 depending on the amount of AOH.

The reported $NH_4V_3Se_2O_{12}$ was synthesized, as rodlike crystals in high yield along with $(NH_4)_2V_6O_6$ crystals as impurity, from a hydrothermal reaction of $V_2O_5/SeO_2/NH_4Cl$ = 3.3/9/18.7 (mmol) in 17 mL of H_2O at pH 5 and 200 °C. The pH of the solution was adjusted by adding NH_4OH before the reaction. A pure $NH_4V_3Se_2O_{12}$ phase was synthesized when more SeO_2 was used with $V_2O_5/SeO_2/NH_4Cl$ = 3.3/10.8/18.7 (mmol). For comparison's sake, we have included this system in our study. We could synthesize the same phase from a $V_2O_5/SeO_2/NH_4OH$ = 5/15/5 (reaction A-1, Table 1) reaction at 200 °C but with some unidentified impurity. However, when the same reaction was run at 230 °C, we could obtain a pure $NH_4V_3Se_2O_{12}$ phase (reaction A-2). A similar observation of increased purity at higher reaction temperature was made with A = K (see below)

The A = Rb and Cs systems showed results almost similar to each other. When the $V_2O_5/SeO_2/AOH$ ratio was 5/15/5 (reactions R-1 and C-1), both systems produced pure pale greenish yellow powders of $AV_3Se_2O_{12}$ phases. As the amount of AOH was increased (x = 10), yellow powders started to form in both cases (reactions R-2 and C-2, 3). When x was 15 or 20, the products were intimate mixtures of bright yellow platelike crystals and orange microcrystals (reactions R-3 and C-3). The yellow crystals could be isolated by hand, and the ones with A = Cs were analyzed through single-crystal X-ray diffraction techniques, yielding the composition $CsVSeO_5$. The crystals from the Rb-containing reactions have the same crystal structure (see below). Identifications of the orange microcrystals were not pursued because they were intimately mixed with the $AVSeO_5$ crystals. According to the paper on $NH_4V_3Se_2O_{12}$, in which failed attempts to obtain alkali-metal analogs are also reported,[6] these orange compounds should be $A_2V_6O_6$ (A = Rb, Cs).[14] Under these reaction conditions of high AOH contents, the final solution pH was 6−7. According to the Pourbaix diagram for selenium,[15] the selenite (SeO_3^{2-}) is unstable with respect to oxidation into selenate (SeO_4^{2-}) in this pH range. Since the selenate ion generally behaves very much like the sulfate ion and thus probably remains in the solution,[16] the formation of the selenium-free $A_2V_6O_6$ phases can be understood as resulting from the oxidation reaction of the selenite.

Within the V_2O_5/SeO_2 = 5/15 series in 10 mL of H_2O, we could not determine the right mole ratio where pure $AVSeO_5$ phases were formed. Instead, when the V_2O_5 content was lowered to $V_2O_5/SeO_2/AOH$ = 3/15/x mmol, we could synthesize pure $RbVSeO_5$ with x = 10 (reaction R-5) and $CsVSeO_5$ with x = 15 (reaction C-5). In this series, the increase of AOH content again resulted in $A_2V_6O_6$ impurities (reactions R-6 and C-6). A pure $RbV_3Se_2O_{12}$ phase was also synthesized with x = 5 (reaction R-4).

In the K-containing system, the $V_2O_5/SeO_2/KOH$ = 5/15/5 (reaction K-1) reactions repeatedly produced pure greenish yellow hexagonal rodlike crystals of $KV_3Se_2O_{12}$. The crystals were generally large, and their sizes could be increased up to 1.5 × 1.5 × 4 mm when the reactions were run for longer periods or when seed crystals were present. The reaction yields were typically over 95% based on vanadium metal. In contrast, lower temperature reactions at 200 °C of the same composition (reaction K-2) produced impure $KV_3Se_2O_{12}$. Observations in this and the NH_4-containing systems indicate that the reaction temperature is important for the syntheses of pure products. With more KOH (x = 10, 15) in the solution, this system showed behavior completely different from those of heavier congeners; there started to form a red brown mudlike mass whose amount increased with the increase of the starting KOH content (reactions K-3 and K-4). This mudlike material gave a powder pattern too low in quality to allow phase identification. Reactions with lower V_2O_5 content (reactions K-5 and K-6) did not make much change in the type of phase formed.

(13) Pope, M. T. *Heteropoly and Isopoly Oxometalates*; Springer-Verlag: New York, 1983.

(14) Range, K.-J.; Eglmeier, C. *Z. Naturforsch.* **1989**, *45B*, 31.

(15) Pourbaix, M. J. N. *Atlas of Electrochemical Equilibria in Aqueous Solution*; Pergamon: New York, 1966.

(16) Cotton, F. A.; Wilkinson, G. *Advanced Inorganic Chemistry. A Comprehensive Text*, 4th ed.; John Wiley & Sons: New York, 1980: p 533.

The Na-containing reactions did not produce any indentifiable phases regardless of many trials with various NaOH contents. When the NaOH content was high, the product was a brown mudlike mass similar to that from the high KOH content reactions. No further attempt was made in this system.

It should be emphasized at this point that the $AV_3Se_2O_{12}$ phases could be synthesized in high purity for A = K, Rb, and Cs as well as NH_4 when the right reaction conditions were chosen, which is in a sharp contrast to the reported failure.[6] In the reported reactions, $A_2V_6O_6$ compounds were the only products for alkali metals. The major difference between the reported preparations and ours is the reaction temperature and the pH. The temperature effects were seen in the A = NH_4 and K cases where the 230 °C reactions resulted in higher yields and purity than the 200 °C reactions. However, the temperature alone did not determine the type of major phase in the product. Even though not mentioned explicitly in the report, the unsuccessful syntheses for $AV_3Se_2O_{12}$ with alkali metals seem to have been attempted with pH adjustment as in the $NH_4V_3Se_2O_{12}$ synthesis, reflecting the authors' discussion on the importance of pH. However, as discussed above, V_2O_5 dissolution into acidic solution results in an increase of pH. If the pH of the starting solution is adjusted to 5, the final pH must rise beyond 7, where selenite is completely oxidized to selenate. The fact that only $A_2V_6O_6$ phases have been obtained in the reported study can be explained by the above reasoning. The exception for the ammonium case, as correctly pointed out in the paper, can be explained by the buffer action of ammonium that maintained the pH around 5. On the other hand, our syntheses started in very acidic solutions and the final pH reached between 3 and 6, where selenite was stable with respect to oxidation reactions.

The material balances in the solutions also appear to be important for the types of phases formed. The $AV_3Se_2O_{12}$ phases were formed when the AOH/V_2O_5 ratios were 5/5 or 5/3 while the $AVSeO_5$ phases were formed when these ratios were 15/5 or 10/3. Although not exactly proportional, the mole ratios of the products follow those in the solutions.

We have also attempted reactions including Et_4NCl. A $V_2O_5/SeO_2/Et_4NCl$ = 3/15/10 reaction at 230 °C for 3 d yielded pure dark green platelike crystals which turned out to be the reported $VOSeO_3 \cdot H_2O$. [5] This V(IV) compound was reportedly obtained, along with metallic Se, from a 1/3 hydrothermal reaction of V_2O_5 and H_2SeO_3 at 200 °C. However, the reaction cannot take place as described because there is no reducing agent to produce selenium metal from H_2SeO_3 and V(IV) from V_2O_5. In contrast, our synthesis of $VOSeO_3 \cdot H_2O$ can be well accounted for through the reduction of V_2O_5 and SeO_2 by $(C_2H_5)_4N^+$. Therefore, we believe that the reported synthesis is in error and that the correct reaction conditions should include a reducing agent as in our $V_2O_5-SeO_2-(C_2H_5)_4NCl$ combination.

Crystal Structure. $(NH_4)V_3Se_2O_{12}$ crystallizes in the noncentrosymmetric space group $P6_3$.[6] The structure can be described as layers of $[V_3Se_2O_2]^-$ in the *ab* plane of the hexagonal unit cell and A cations between the layers (Figure 1). Each layer has vanadium oxide octahedra that share corners to form six-membered rings. The selenite groups cap three corner- sharing vanadium oxide octahedra above and below the layer. The interlayer alkali metal cations are more or less nested inside the vanadium oxide six-membered rings from only one side (from the $+c$ direction in Figure 1) of the layer. In fact, this arrangement of the alkali metals with respect to the layer is the only factor that makes the structure noncentrosymmetric. Our synthesis results show that alkali metals (A = K, Rb, Cs) can be incorporated into the ammonium position of this layered structure. The powder patterns of these compounds are shown in Figure 2.

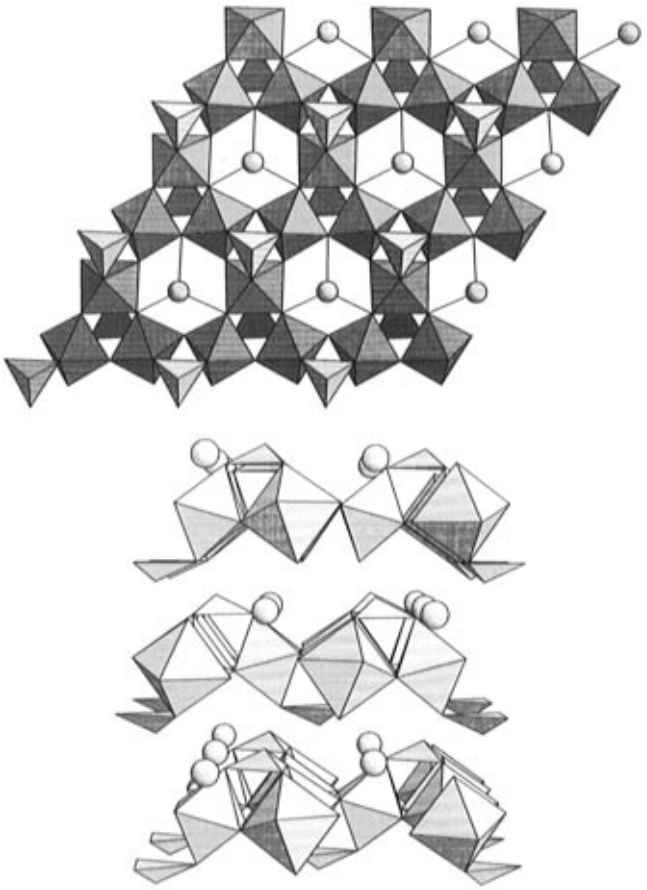

Figure 1. Structure of $NH_4V_3Se_2O_{12}$: (a) (top) viewed along the (−)-*c*-direction; and (b) (bottom) viewed perpendicularly to the *c* axis.

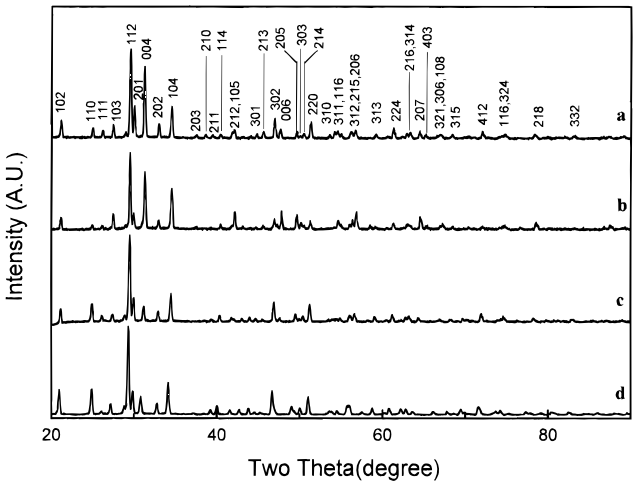

Figure 2. Powder patterns for (a) $NH_4V_3Se_2O_{12}$, (b) $KV_3Se_2O_{12}$, (c) $RbV_3Se_2O_{12}$, and (d) $CsV_3Se_2O_{12}$.

The $CsVSeO_5$ structure is completely different from that of $AV_3Se_2O_{12}$. The structure has VO_5 pentahedra and SeO_3 trigonal pyramids that share corner oxygens to form a three-dimensional network (Figure 3). Cesium metals fill the empty space of this network. Figure 4 shows the asymmetric unit and the numbering scheme for the structure.

Many of V(V) oxo compounds show (distorted) octahedra or tetrahedra, but there are quite a few examples in which vanadium(V) is coordinated to five oxygens. Ideally, five-coordinations should have trigonal bipyramid or square pyramid

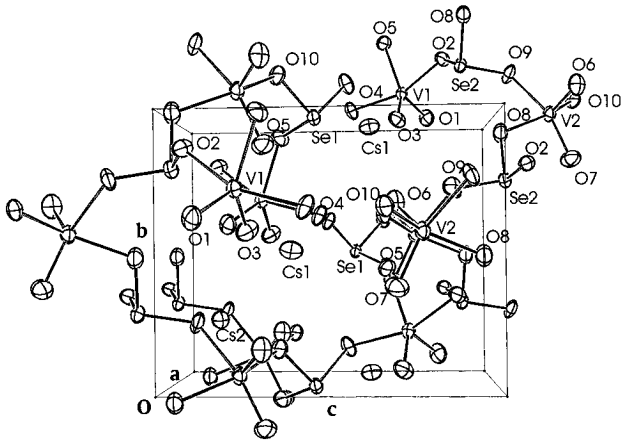

Figure 3. Structure of $CsVSeO_5$ viewed in the [010] direction.

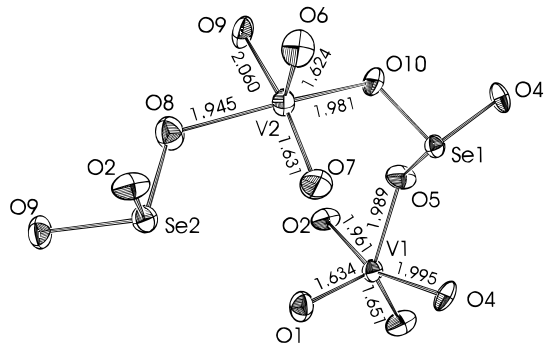

Figure 4. Asymmetric unit and labeling scheme for $CsVSeO_5$. Important V−O bond distances are shown.

structures or a hybrid of these two.[17] However, the pentahedra found in the present structure deviate from any of these ideal structures. The VO_5 geometry for V(1) is more or less like that of $KVO_3 \cdot H_2O$, where the oxygens are arranged in a distorted trigonal bipyramid structure.[18] In the $KVO_3 \cdot H_2O$ structure, there are two short symmetry-related (1.63 Å) and one long (1.99 Å) V−O bonds in the equatorial plane of the trigonal bipyramid. The two equivalent axial V−O bonds with V−O distances of 1.93 Å are tilted toward the long equatorial V−O bond direction. Because of these distortions, the trigonal pyramid loses its 3-fold rotation symmetry but preserves its mirror planes. In $CsVSeO_5$, the VO_5 pentahedron for V(1) is further distorted. There is no symmetry element that relates the oxygen atoms. There are two short (1.634(6) and 1.651(6) Å) and one long (1.989(6) Å) V−O bonds in the equatorial plane and two long (1.961(6) and 1.995(5) Å) V−O bonds in the pseudoaxis of the distorted trigonal bipyramid. The local geometry for this unit can be found at the bottom right of Figure 4.

The VO_5 unit for V(2) is different from that for V(1). Similar oxygen geometry of V(V) can be found in the $VOPO_4$ structure,[19] in which the VO_5 geometry can be described as a distorted square pyramid. In $VOPO_4$, there are four symmetry-related oxygens with V−O distances of 1.87 Å forming the square base of the pyramid and an apical oxygen with a short V−O distance of 1.58 Å. The VO_5 of V(2) in $CsVSeO_5$ has two short and three long V−O bonds. One of the two short bonds is the apical one of V(2)−O6 (1.624(6) Å), and the other is the one with O7 in the base of the square pyramid (V(2)−O7, 1.631(7) Å). The O−V−O bond angles around O6 are close to one another in the range 102.9(3)−106.6(4)°, but those around O7 range from 92.0(3) to 150.2(3)°. Both VO_5 pentahedra of V(1) and V(2) have two short and three long V−O bonds. The three oxygens of long bonds are bridges to neighboring selenium atoms and the two of short bonds are terminal ones.

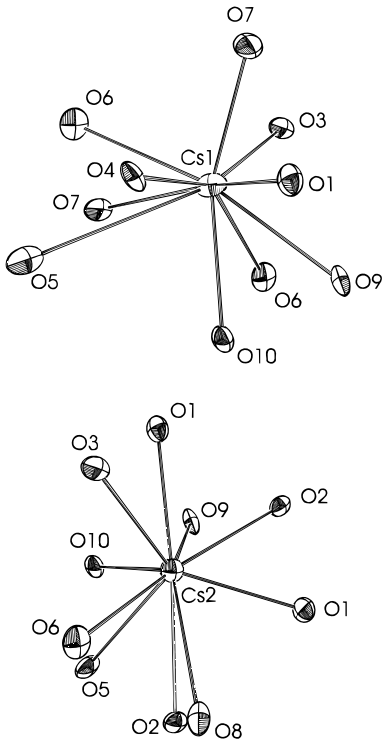

Figure 5. Oxygens surroundings for (a) (top) Cs(1) and (b) (bottom) Cs(2) of $CsVSeO_5$.

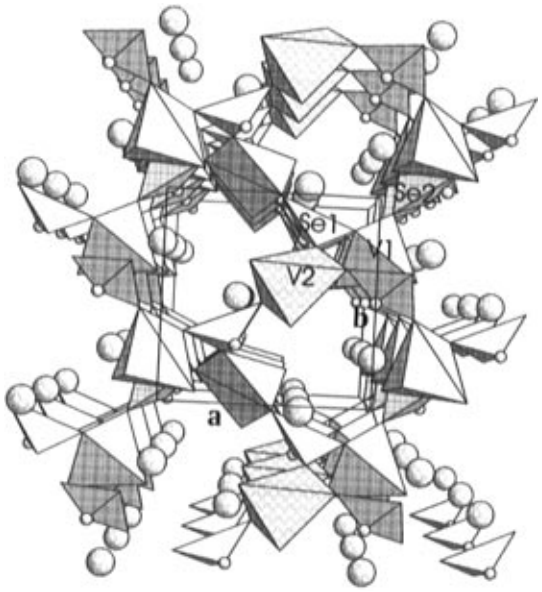

Figure 6. Polyhedral drawing for $CsVSeO_5$ viewed in the [010] direction. Polyhedra are labeled as the central atoms. The small circles on the SeO_3 trigonal pyramids are selenium atoms to show the orientation of the pyramids.

There are two different cesium atoms (Figure 5). Each of Cs atoms is surrounded by 10 oxygen atoms with Cs−O distances ranging from 3.028 to 3.765 Å for Cs(1) and from 3.082 to 3.672 Å for Cs(2). The nonbridging oxygens of both VO_5 pentahedra participate in the coordination to Cs atoms more

(17) Muetterties, E. L.; Guggenberger, L. *J. Am. Chem. Soc*. **1974**, *96*, 1748.
(18) Wells, A. F. *Structural Inorganic Chemistry*, 5th ed.; Clarendon Press; Oxford, U.K., 1984; p 568.
(19) Jordan, B.; Calvo, C. *Can. J. Chem.* **1973**, *51*, 2621. Gopal, R.; Calvo, C. *J. Solid State Chem.* **1972**, *5*, 432.

Table 5. Calculated Lattice Parameters for $AV_3Se_2O_{12}$ and $AVSeO_5$ Compounds

compd	A	*a*(Å)	*b*(Å)	*c*(Å)	β (deg)	*V* (Å^3)	remark
$AVSeO_5$	Rb	7.646(2)	7.681(2)	9.367(2)	93.18(2)	549.3(1)	this work
	Cs[a]	7.887(3)	7.843(2)	9.497(3)	92.13(3)	587.1(3)	this work, single crystal
$AV_3Se_2O_{12}$	NH_4[b]	7.122(1)		11.445(2)		502.8(1)	this work
		7.137(3)		11.462(4)		505.7(4)	ref 6
	K	7.1281(8)		11.415(1)		502.3(1)	this work
	Rb	7.1405(7)		11.476(2)		506.7(1)	this work
	Cs	7.1581(7)		11.608(2)		515.08(9)	this work

[a] Monoclinic unit cell, space group $P2_1$. [b] Hexagonal unit cell, space group $P6_3$.

extensively than the other ones. Of the ten coordinating oxygen atoms, six are vanadyl oxygens for Cs(1) and four are for Cs-(2).

The bond valence sum calculations[20] for this structure resulted in 4.937 for V(1), 5.00 for V(2), 4.077 for Se, 4.045 for Se(2), 1.136 for Cs(1), and 1.149 for Cs(2), which are close to the corresponding ideal values of 5, 4, and 1 for V, Se, and Cs, respectively, for the compound charge balance $Cs^{I}V^{V}Se^{IV}O^{-II}_5$.

The three-dimensional network structure in Figure 3 is rather complex. Since two of the five oxygens of the VO_5 unit are not shared, the VO_5 group can be considered a structural motif similar to SeO_3. These alternating structural motifs form spires in all three directions. Better grasp of the structure can be gained by polyhedra packings shown in Figure 6, a view along the (−)*b* direction. This figure shows a left-handed screwlike spiral arrangement of seemingly 8-membered rings composed of alternating O−O edges of VO_5 and SeO_3 units or 16-membered rings counting metal and oxygen atoms individually. Along the *a* and *c* axes, the structure also shows left- and right-handed 8-membered spiral structures, respectively. The powder pattern for the $RbVSeO_5$ compound can be readiliy accounted for by using $CsVSeO_5$ structural data but with smaller lattice parameters.

The lattice parameters for $AV_3Se_2O_{12}$ and $AVSeO_5$ compounds are given in Table 5. The lattice parameters for our $NH_4V_3Se_2O_{12}$ compound are smaller than those reported even though the differences are within experimental errors. Their values are rather close to those of our Rb compound. The overall trend of lattice parameters with cation size is more favorable for our data.

The variations of the unit cell volume (Figure 7a) and the cube root of the unit cell volume per formula unit (Figure 7b) for both $AV_3Se_2O_{12}$ and $AVSeO_5$ series are plotted against the Shannon's cation radii.[21] The two series of compounds show much different trends in both plots. The unit cell volumes in the $AV_3Se_2O_{12}$ compounds are nearly constant while those in the $AVSeO_5$ compounds increase considerably with cation size (Figure 7a). The slope of the plot in Figure 7b can be interpreted as how well the cation size is reflected in the lattice volume. When the unit cell volume fully reflects the atom size change, this value should be unity; a value smaller than unity means that the crystal lattice absorbs part of the volume increment due to the cation size increase. The slopes are 0.183 and 0.787 for the $AV_3Se_2O_{12}$ and $AVSeO_5$ series, respectively. The latter value is closer to 1, and the lattice volume reflects the cation size better than the former. However, the slope of 0.183 for the $AV_3Se_2O_{12}$ series indicates that the cation size effect is heavily attenuated by the crystal structure. As mentioned above for the crystal structure of $NH_4V_3Se_2O_{12}$, the cations are nested inside the six-membered rings of vanadium oxide which is already empty. This nesting of cations probably can explain the smaller slope for this compound series than for the $AVSeO_5$ one. Such different environments for the cations are likely

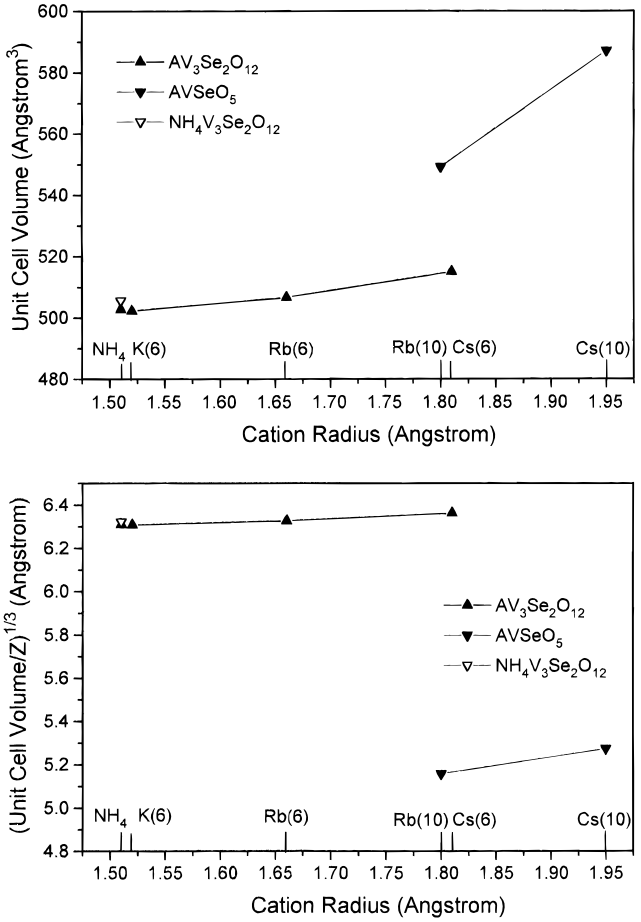

Figure 7. Variations of (a) (top) unit cell volume vs cation radius and (b) (bottom) (unit cell volume/Z)$^{1/3}$ vs cation radius. The ionic radii for the cations are shown on the horizontal axis. The numbers in parentheses are the coordination numbers.

related to the range of cations that can be incorporated into the given structure types. As pointed out above, the $AV_3Se_2O_{12}$ structure appears to be relatively insensitive to cation size. Thus, a wide range of cations ranging from K to Cs can be incorporated into this structure. However, Na may be too small to stabilize this structure, rationalizing our inability to synthesize this compound. In contrast, for the $AVSeO_5$ structure, large cations seem to be essential to support the framework of the structure, and thus this structure is found only for A = Rb and Cs.

Infrared Spectroscopy. The infrared spectra show characteristic absorption peaks for each group of compounds (Table 6). Unfortunately, the literature on transition metal selenites and V(V) oxo compounds does not provide unified peak assignments of their infrared spectra. Therefore, we do not attempt to assign peaks for our IR data but refer to the reported assignments for $NH_4V_3Se_2O_{12}$. Besides the peaks due to NH_4^+, the reported infrared spectrum for $NH_4V_3Se_2O_{12}$ showed peaks at 941, 812, and 689 cm^{-1}. The first peak was assigned to SeO_3^{2-}, and the last two were assigned to symmentric and

(20) Brown, I. D.; Altermatt, D. *Acta Crystallogr.* **1985**, *B41*, 244.
(21) Shannon, R. *Acta Crystallogr.* **1976**, *A32*, 751. Shannon, R.; Prewitt, C. T. *Acta Crystallogr.* **1969**, *B25*, 925.

Table 6. Infrared Spectral Data (cm^{-1}) for $AV_3Se_2O_{12}$ and $AVSeO_5$ Compounds

	$AV_3Se_2O_{12}$					$AVSeO_5$	
assign[a]	A = NH_4		A = K	A = Rb	A = Cs	A =Rb	A = Cs
$\nu(NH_4)$	1421 m	1420 s					
$\nu(SeO_3^{2-})$	941 w	940 w	945 w	943 w	943 w	955 s	947 s
		913 sh	907 sh	912 sh	907 w	896 s	947 s
$\nu_s(VO_6)$	812 vs	825 vs	799 vs	823 vs	817 vs	832 m	833 s
		720 sh	731 sh	727 sh	729 sh	715 vs[b]	710 vs[b]
$\nu_{as}(VO_6)$	689 s	690 s	685 s	690 s	692 s		
						561, 574 s	567 s
						510 m	502 m
		490 m	490 m	490 m	497 m	475 w	477 w
		435 m	437 m	433 m	435 m	430 s	431 m
remarks	ref 6	this work	this work	this work	this work	this work	this work

[a] Assignments as given in ref 6. [b] These peaks are very broad over 140−150 cm^{-1} centered at these values. There are also many unresolved features in these peaks.

asymmetric stretching modes of the VO_6 octahedra, respectively. Our $AV_3Se_2O_{12}$ compounds show corresponding peaks in the 940−943, 799−825, and 685−692 cm^{-1} ranges. There are a few additional peaks at 907−913, 720−731, 490−497, and 433−437 cm^{-1} that are not in the reported spectrum for $NH_4V_3Se_2O_{12}$. As discussed in the above paper, the first two groups of peaks may well be assigned to SeO_3^{2-} while the two low-frequency peaks may be due to the bending modes.

The infrared spectra for $RbVSeO_5$ and $CsVSeO_5$ show peaks in the same frequency range as for $AV_3Se_2O_{12}$ and a few more in the 500−574 cm^{-1} range. In Table 6, we report only the peak positions of each compound and the reported assignments for $NH_4V_3Se_2O_{12}$.

Conclusion

We have studied the hydrothermal reactions of V_2O_5 and SeO_2 with alkali metal and ammonium ions under various reaction conditions. The reaction products show strong dependency on the mole ratio of the reagents, on pH, and slightly on the reaction temperature. By controlling these parameters, we have synthesized pure $AV_3Se_2O_{12}$ (A = K, Rb, Cs, NH_4) and $AVSeO_5$ (A = Rb, Cs) compounds. The compounds in the first group are isostructural with $(NH_4)V_3Se_2O_{12}$, a phase reported earlier, and the latter group exhibits a new structure type.

Acknowledgment. We thank Prof. H. Namgung, Kookmin University, Seoul, Korea, for the X-ray single-crystal diffraction data collection. This research was funded by the Korean Science and Engineering Foundation (Grant KOSEF 93-0300-012-2).

Supporting Information Available: Tables of crystal data, thermal parameters, and bond distances and angles for $CsVSeO_5$ and tables of powder diffraction data for $RbVSeO_5$ and $AV_3Se_2O_{12}$ (A = K, Rb, Cs) (16 pages). Ordering information is given on any current masthead page.

IC9509488